



Article

Identification Method and Quantification Analysis of the Critical Aging Speed Interval for Battery Knee Points

Xinyu Jia ^{1,2,3} , Caiping Zhang ^{1,*}, Linjing Zhang ¹, Weige Zhang ¹ and Zhongling Xu ³

¹ National Active Distribution Network Technology Research Center (NANTEC), Beijing Jiaotong University, Beijing 100044, China; xinyu.jia@bjtu.edu.cn (X.J.); lj.zhang@bjtu.edu.cn (L.Z.); wg.zhang@bjtu.edu.cn (W.Z.)

² School of Materials Science and Engineering, South China University of Technology, Guangzhou 510641, China

³ Sunwoda Mobility Energy Technology Co., Ltd., Shenzhen 518107, China; xuzhongling@sunwoda-evb.com

* Correspondence: zhangcaiping@bjtu.edu.cn

Abstract: The identification of knee points in lithium-ion (Li-ion) batteries is crucial for predicting the battery life, designing battery products, and managing battery health. Knee points (KPs) refer to the transition points in the aging speed and aging trajectory of Li-ion batteries. KPs can be identified using a wealth of aging data and various regression-based methods. However, KP identification relies on a large amount of aging data, which is exceedingly time-consuming and resource-intensive. To overcome this issue, we propose a novel method based on KP characteristics to identify the KPs and critical aging speed. Firstly, we extract the main aging trajectory using curve-fitting techniques. Secondly, we calculate the aging speed at each cycle to identify the KPs. We then explore the relationship between the KPs and cycle life and develop a knee point identification algorithm. The correlation coefficient between the KPs and cycle life provides a valuable indicator of the critical aging speed, enabling accurate identification of KPs. To validate our approach, we apply it to the Li(NiCoMn)O₂, LiFePO₄, and LiCoO₂ cell datasets. Our results demonstrate a strong correlation between the KPs and cycle life for these battery types. By employing our proposed method, KPs can be identified for battery life prediction, product design, and health management. Moreover, we summarize a critical degradation speed of $-0.03\%/cycle$ can serve as an empirical threshold for warning against capacity diving and KPs. The statistical transition speed threshold can eliminate the dependence on extensive aging data throughout the entire battery's lifecycle for identifying capacity knee points.

Keywords: lithium-ion battery; accelerated aging; knee point identification; critical aging speed interval; battery cycle life; battery safety and health



Citation: Jia, X.; Zhang, C.; Zhang, L.; Zhang, W.; Xu, Z. Identification Method and Quantification Analysis of the Critical Aging Speed Interval for Battery Knee Points. *World Electr. Veh. J.* **2023**, *14*, 346. <https://doi.org/10.3390/wevj14120346>

Academic Editors: Rongheng Li and Xuan Zhou

Received: 6 November 2023

Revised: 4 December 2023

Accepted: 6 December 2023

Published: 12 December 2023



Copyright: © 2023 by the authors. Licensee MDPI, Basel, Switzerland. This article is an open access article distributed under the terms and conditions of the Creative Commons Attribution (CC BY) license (<https://creativecommons.org/licenses/by/4.0/>).

1. Introduction

During the operation of lithium-ion batteries, a phenomenon known as a knee point may occur. When the battery reaches this knee point, there is a rapid decline in capacity, which accelerates the aging process and poses potential safety risks [1,2]. Accurately identifying and predicting knee points is of great importance for ensuring the safe and economical use of batteries [3]. Additionally, capacity diving is a crucial factor to consider in the control strategy of electric vehicles [4]. In terms of predicting the battery lifespan, taking knee points into account can enhance the accuracy of aging trajectory predictions based on machine learning techniques [5].

The accelerated aging mechanism of lithium-ion batteries encompasses several factors, including the loss of positive and negative electrode active materials, lithium-ion loss, and increased internal resistance [6]. High discharge rates can accelerate battery aging, with the capacity degradation speed of lithium-ion batteries increasing as the discharge rate rises. Additionally, as the discharge rate increases, the aging mechanism of lithium-ion batteries changes [7]. Weiping Diao et al. [8] discovered, using incremental capacity analysis and

destructive analysis, that an increase in the positive electrode internal resistance can lead to capacity diving in batteries. Xiaoguang Yang et al. [9] observed that the thickening of the solid electrolyte interphase (SEI) film during lithium-ion aging not only resulted in a decrease in the negative electrode porosity but also triggered lithium evolution. This lithium evolution further contributed to a decrease in the negative electrode porosity, thereby exacerbating the extent of lithium evolution. Throughout this process, the reduced porosity of the negative electrode and separator led to a significant increase in the battery's internal resistance. Yang Gao et al. [10] identified that the mechanism behind battery capacity diving primarily involves the loss of active materials and lithium plating, with high temperatures and discharge rates significantly increasing the likelihood of accelerated aging.

Currently, machine learning and deep learning techniques are widely employed for predicting knee points in battery capacity [11]. Saurabh Saxena et al. [12] proposed a method based on convolutional neural networks to predict the knee point of lithium-ion battery capacity. Weihan Li et al. [13] introduced a deep-learning-based approach for battery health diagnosis, enabling the prediction of knee points in a single shot without the need for iteration or feature extraction. Samuel Greenbank et al. [14] proposed a data-driven method that utilizes automated feature selection to generate inputs for a Gaussian process regression model, which predicts knee points. Paula Fermín Cueto et al. [15] used the Bacon and Watts model and a battery capacity decay curve to identify capacity diving points and predicted knee points using machine learning. They also discovered a strong correlation between knee points and the cycle life of LiFePO₄ (LFP) batteries. Caiping Zhang et al. [16] proposed a method that combines quantile regression with Monte Carlo simulation to achieve online recognition of knee points in accelerated aging batteries. Weiping Diao et al. [17] utilized the slope change rate and the two tangent lines of the capacity decay curve to identify battery knee points. While knee point prediction in capacity diving aims to determine whether rapid capacity decay will occur at the current moment, the capacity knee point represents a turning point in the speed of battery capacity decay [18]. In ref. [1], Bacon–Watts, Kneedle, bisector, and tangent ratio methods were used to identify the battery knee points. The Bacon–Watts, Kneedle, bisector, and tangent ratio methods mainly focus on the shape of the aging curve's transition points, and they lack attention to the capacity decay speed at the capacity knee point. However, the current identification methods for capacity knee points heavily rely on a large amount of capacity aging data and curve fitting, lacking a critical aging speed interval threshold suitable for detecting knee points in lithium-ion batteries of different material systems. Consequently, the identification of battery capacity knee points relies on a substantial amount of historical aging data and faces challenges in online identification. Unlike the Bacon–Watts, Kneedle, bisector, and tangent ratio methods in ref. [1], the knee point identification method proposed in this paper targets the correlation between the capacity knee points and cycle life as the search criterion for the critical aging rate in knee point identification. Therefore, the identified capacity knee points correspond to the inflexion points in the accelerated aging battery's decay curve, and these capacity knee points hold significant importance for predicting battery cycle life.

To address the challenge of identifying battery capacity knee points, this paper collected accelerated aging data for Li(NiCoMn)O₂ (NCM) batteries, LFP batteries, and LiCoO₂ batteries. Subsequently, the correlation between the capacity knee point and the cycle life of accelerated aging batteries was analyzed. Building upon the strong correlation observed between the capacity knee point and the cycle life of accelerated aging batteries, a critical aging speed range and a capacity knee point identification method for accelerated aging batteries are proposed. Additionally, the critical aging speed range for the capacity diving of NCM batteries, LFP batteries, and LiCoO₂ batteries was analyzed, providing a valuable foundation for safety warnings regarding the accelerated aging of batteries, even in the absence of a large amount of historical aging data. The structure of this paper is organized as follows: Section 2 presents the cycle life experiences and results of the battery. Section 3 introduces the critical aging speed range and the capacity knee point identification method.

Section 4 presents the discussion and identification results of the capacity knee point and the critical aging speed range. Finally, Section 5 summarizes the conclusions of this paper.

2. Cycle Life Test and Battery Aging Datasets

In the process of lithium-ion battery degradation, capacity diving occurs at uncertain times, making it difficult to predict the emergence of knee points. This section aims to address this issue by collecting cycle aging data from NCM, LFP, and LiCoO₂ batteries, and analyzing the degradation characteristics of accelerated aging batteries across different material systems. The specifications of NCM, LFP, and LiCoO₂ batteries are summarized in Table 1. The NCM battery dataset includes 114 Ah and 36 Ah NCM batteries. The charging and discharging cut-off voltage of the 114 Ah NCM batteries are 4.25 V and 2.8 V. The charging and discharging cut-off voltage of the 36 Ah NCM batteries are 4.15 V and 2.5 V.

Table 1. Nominal specifications of the batteries.

Item	NCM	LFP	LiCoO ₂
Cathode material	Li[Ni _x Co _y Mn _{1-x-y}]O ₂	LiFePO ₄	LiCoO ₂
Anode material	Graphite	Graphite	Graphite
Nominal capacity	114 Ah, 36 Ah	1.1 Ah	5 Ah
Charging cut-off voltage	4.25 V (114 Ah) 4.15 V (36 Ah)	3.6 V	4.48 V
Discharging cut-off voltage	2.8 V (114 Ah) 2.5 V (36 Ah)	2 V	3 V

From a pool of 36 aging NCM batteries in IEEE DataPort (DOI: 10.21227/gnst kz81), 19 accelerated aging NCM batteries were selected to analyze their knee points in this paper. The NCM battery dataset can be found at '<https://iee-dataport.org/documents/early-diagnosis-accelerated-aging-lithium-ion-batteries-integrated-framework-ageing>' (accessed on 27 August 2022). The 36 NCM data were collected and published in [19] for analyzing aging mechanisms and accelerated aging diagnosis. These batteries utilized graphite as the negative electrode material and were subjected to cycling at various temperatures and discharge rates. The specific cycling temperature and discharge current rate for each cell can be found in Table 2. Figure 1 illustrates the cyclic capacity aging trajectory of the 19 accelerated aging NCM batteries. The capacity retention ratio is calculated by dividing the discharge capacity of the *n*th cycle by the discharge capacity of the first cycle. The aging trajectory of these 19 accelerated aging NCM batteries exhibits a significant nonlinearity. In these 19 accelerated aging NCM batteries, batteries 11 and 12 are 114 Ah NCM batteries, and other batteries are 36 Ah NCM batteries.

Table 2. Cycle temperature and discharge current rate of NCM batteries.

NCM Battery Number	Temperature	Discharge Current Rate
11, 12	25 °C	0.5 C
20, 21, 22, 23, 24	25 °C	1 C
25, 26	25 °C	1.5 C
27	25 °C	2 C
28	10 °C	1.5 C
29, 30	35 °C	1 C
31, 32, 33	35 °C	1.5 C
34, 35, 36	45 °C	1 C

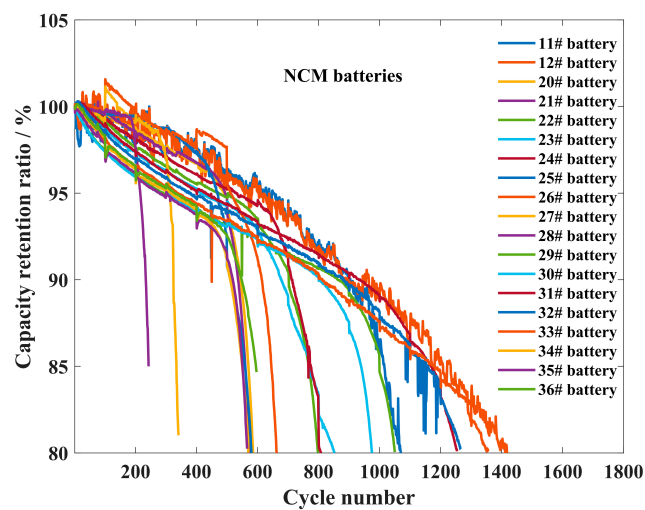


Figure 1. Aging characteristics of accelerated aging NCM batteries under different temperatures and discharge current rates.

Next, we will introduce the LFP battery aging dataset [20]. This dataset consists of aging data from 124 LFP batteries that were cycled until the end of their lifespan. These batteries underwent cycling tests under fast charging conditions. The cyclic testing of the 124 LFP batteries was conducted using the Arbin lithium-ion battery testing equipment at a temperature of 30 °C. The calibration capacity of the LFP batteries used in the testing was 1.1 Ah, and the calibration voltage was set at 3.3 V.

All LFP batteries in this study were subjected to either a first- or second-order fast charging strategy. The format of this strategy is denoted as “C1 (Q1)-C2”, where C1 and C2 represent the battery rate during the first and second constant current fast charging stages, and Q1 represents the state of charge (SOC) during the current switching. Upon reaching an 80% SOC, the battery undergoes a 1 C constant current–constant voltage (CC-CV) charging step, following which all batteries are discharged at a rate of 4 C. The charging and discharging cut-off voltage for these batteries are set at 3.6 V and 2.0 V, respectively. The charging and discharging cut-off voltage are according to the manufacturer’s specifications. Figure 2 illustrates the cyclic capacity decline trajectory of the 123 accelerated aging LFP batteries (excluding one defective battery with a cycle life of less than 200). These 123 LFP batteries are all accelerated aging batteries, and there will be capacity drops and knee points in the process of the LFP batteries’ cycle aging. After the capacity knee point, the cycle capacity of the LFP batteries decreases fast, and the aging rate increases rapidly.

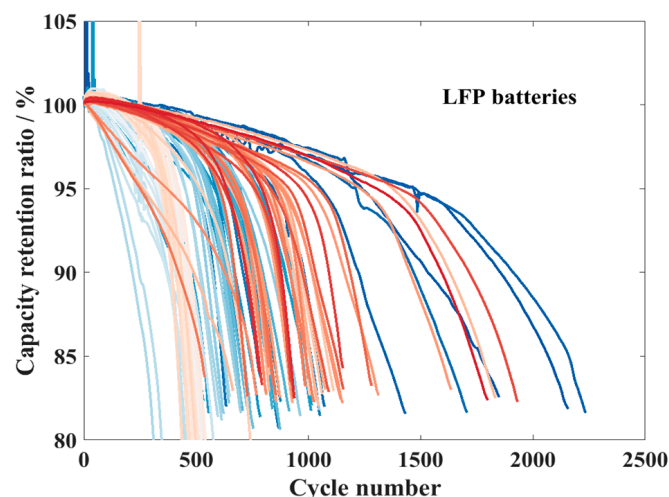


Figure 2. Aging characteristics of accelerated aging LFP batteries under different fast charging strategies.

In contrast to the cycle life experiments conducted on the NCM and LFP batteries under various cycle conditions, the cycle life tests performed on the LiCoO₂ batteries employed consistent cycle conditions. This approach aimed to investigate the impact of the battery production process consistency on the degradation characteristics of the batteries. The LiCoO₂ battery cycle life dataset not only provides data on the cycle aging of lithium-ion batteries with different material systems for this study but also explores whether the battery production process can lead to accelerated aging.

The cycle life test of the LiCoO₂ batteries involved 124 batteries. The cycling test was conducted at a temperature of 25 °C, and the battery manufacturer provided the cycling charging system. The charging system followed a multi-stage constant current and constant voltage charging protocol. Initially, a constant current of 6 A (1.2 C) was applied until the voltage reached 4.25 V, followed by a cut-off current of 1 C. Subsequently, the battery was subjected to constant current and constant voltage charging at 1 C until reaching 4.45 V, followed by a cut-off current of 0.8 C. Lastly, the battery underwent constant current and constant voltage charging at 0.8 C until reaching 4.48 V, followed by a cut-off current of 0.104 C. The battery was allowed to rest for 5 min. For the cyclic discharge system, a constant current discharge of 0.7 C was applied until reaching a cut-off voltage of 3.0 V. All batteries underwent 700 cycles of charging and discharging.

Figure 3 depicts the cyclic capacity aging trajectories of 124 LiCoO₂ batteries, all of which underwent 700 cycles. Among them, 106 LiCoO₂ batteries exhibited an approximately linear decay in their cyclic capacity aging curve, while 18 LiCoO₂ batteries displayed a nonlinear decay. The LiCoO₂ batteries with an approximately linear decay maintained a cycling capacity retention ratio of over 80% after 700 cycles, indicating that they did not reach the end of their lifespan. These batteries exhibited a cycling life exceeding 700 cycles. On the other hand, the LiCoO₂ batteries with nonlinear decay exhibited a cycling capacity retention ratio below 80% and a cycling life of less than 700 cycles. Consequently, this study employed 700 cycles as the threshold to differentiate between normal aging and accelerated aging LiCoO₂ batteries, resulting in 106 normal aging LiCoO₂ batteries and 18 accelerated aging LiCoO₂ batteries. The inconsistency in the battery production process is identified as the cause of accelerated aging in LiCoO₂ batteries, given that all 124 batteries share the same material system and cycling conditions. Enhancing and refining the production process of lithium-ion batteries can mitigate the risk of accelerated aging caused by the battery production process and prolong the lifespan of these batteries.

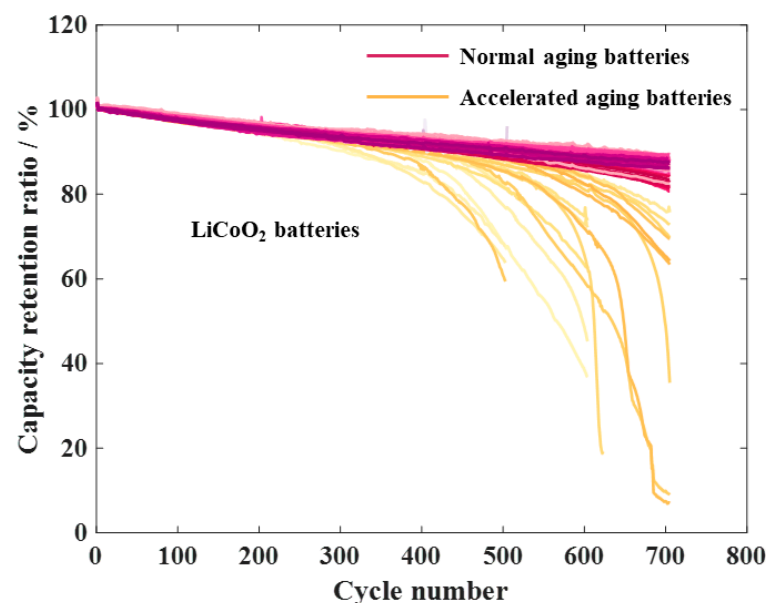


Figure 3. Aging characteristics of accelerated aging and normal aging LiCoO₂ batteries.

3. Identification Method for Critical Aging Speed Range and Knee Points

3.1. Knee Point Characteristics Analysis

As depicted in Figure 4a, the aging rate of 19 NCM accelerated aging batteries is presented. It can be observed from Figure 4b that the aging rate of NCM accelerated aging batteries experiences a rapid increase of approximately -0.025% per cycle. In our previous study [19], we discovered a robust linear relationship between the capacity knee point and cycle life when the aging rate of NCM accelerated aging batteries was around -0.025% per cycle. Similarly, in ref. [15], a strong linear correlation between the capacity knee point and cycle life of LFP batteries was identified using the Bacon–Watts method. Hence, for accelerated aging batteries, there exists a significant association between the capacity knee point and cycle life.

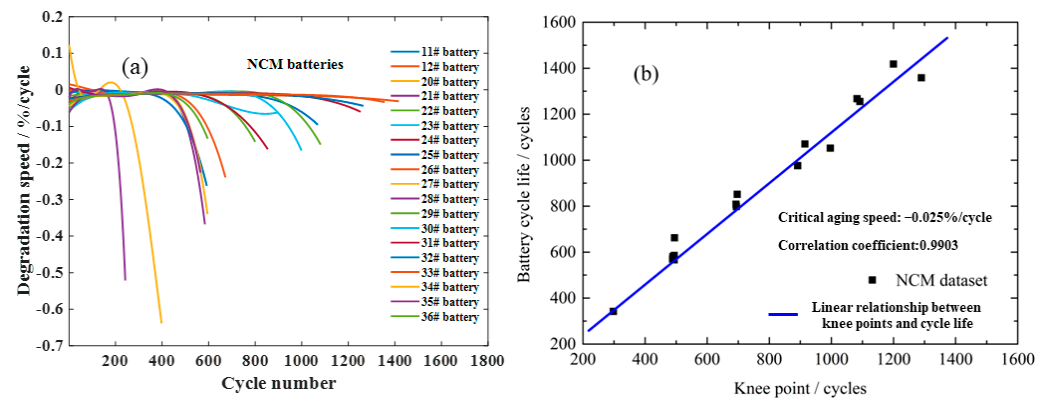


Figure 4. (a) Degradation speed of accelerated aging NCM batteries under different temperatures and discharge current rates; (b) the linear correlation between the KPs and cycle life of accelerated aging NCM batteries.

3.2. Knee Point and Critical Aging Speed Interval Identification Method Based on the Knee Point Characteristics

Based on the analysis presented in the preceding section, it can be observed that employing -0.025% /cycle as the pivotal aging speed, the critical aging rate of accelerated aging batteries not only discriminates between normal and accelerated degradation phases but also exhibits a robust correlation between the capacity knee point corresponding to the critical aging speed and the cycle life. Additionally, a knee point with an aging speed akin to -0.025% /cycle as the critical aging speed may also exhibit a substantial correlation with the cycle life. Therefore, the extraction of capacity diving points necessitates the determination of the critical aging speed range.

Drawing from the definition of critical aging speed and knee points, as well as the key characteristic of a strong correlation between the capacity knee point and cycle life, the optimal critical aging speed range and identification method of capacity knee point, considering the aging characteristics of knee points is shown in Figure 5.

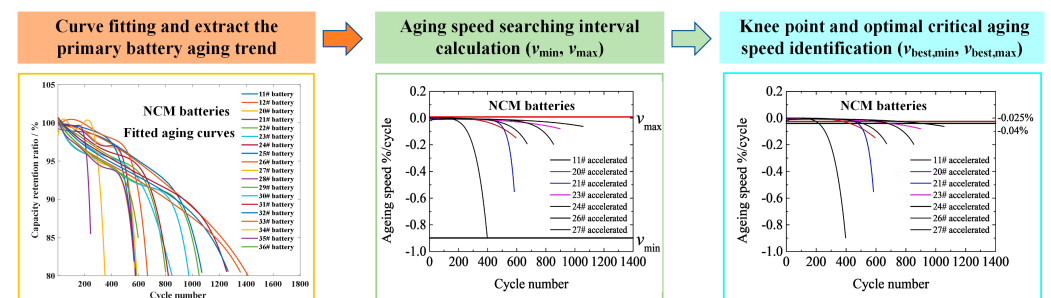


Figure 5. The flow chart of the proposed knee point identification method is based on the knee point characteristic.

The knee point and critical aging speed interval identification method based on the knee point characteristics includes three steps:

Step 1: Initially, employ a polynomial model to fit the capacity aging trajectory curve of the accelerated aging battery, extract the primary decay trend of the battery, and then calculate the aging speed of each cycle for each battery according to Formula (1). Subsequently, calculate the search range for the critical aging speed (v_{\min} , v_{\max}) using Formulas (2) and (3).

$$v_{n,k} = C_{\text{dis},n-1,k} - C_{\text{dis},n,k} \quad (1)$$

$$v_{\max} = \max(v_{n,k}) \quad (2)$$

$$v_{\min} = \min(v_{n,k}) \quad (3)$$

Among them, n is the number of cycles, k is the battery sample number, and $C_{\text{dis},n,k}$ and $C_{\text{dis},n-1,k}$ are the capacity retention ratio of the k th battery on the n cycle and $n-1$ cycle, respectively. $v_{n,k}$ is the aging speed of the k th battery during the n th cycle. v_{\max} is the maximum value of the aging speed of all batteries in the dataset, and v_{\min} is the minimum value of the aging speed of all batteries in the dataset.

Step II: Within the search range of critical aging speed (v_{\min} , v_{\max}), select a specific critical aging speed. The first time, we select the minimum aging speed v_{\min} as the critical speed to obtain the knee points of the accelerated aging batteries. Solve to obtain the number of cycles at which each battery's aging speed equals the selected critical aging speed; this is the capacity knee point of each accelerated aging battery. Subsequently, calculate the correlation coefficient between the extracted capacity knee point and cycle life of the M accelerated aging batteries using Formula (4). If the correlation coefficient exceeds the correlation coefficient threshold (correlation coefficient threshold > 0.9), the chosen critical aging speed will be designated as the optimal critical aging speed v_{best} .

$$r = \frac{\sum_{k=1}^M (KP_k - \overline{KP}) \cdot (CL_k - \overline{CL})}{\sqrt{\sum_{k=1}^M (KP_k - \overline{KP})^2} \cdot \sqrt{\sum_{k=1}^M (CL_k - \overline{CL})^2}} \quad (4)$$

Among them, KP and M are the capacity knee point and the total number of samples of the accelerated aging battery, CL is the cycle life of the accelerated aging battery, k is the sample number, v_{KP} is the aging speed at the capacity knee point, and r is the correlation coefficient between the capacity knee point and the cycle life of the accelerated aging battery. When the absolute value of the correlation coefficient approaches 1, this indicates a strong correlation between the capacity knee point and the battery cycle life. This means that the capacity knee point determines the duration of the battery's cycle life and is a crucial basis for predicting battery life.

Step III: Within the critical aging speed search range (v_{\min} , v_{\max}), repeat step II by continuously adding a certain amount of additional decay rate (e.g., -0.005% /cycle) to the critical aging speed selected previously to obtain a new critical aging speed. Extract the capacity knee points based on the selected critical aging speeds, and then determine the optimal critical aging speed based on whether the correlation coefficient between the capacity knee points and cycle life exceeds the correlation coefficient threshold. After traversing the entire critical aging speed search range (v_{\min} , v_{\max}), we can obtain a set of w optimal critical aging speeds, denoted as $\{v_{\text{best},1}, v_{\text{best},2}, \dots, v_{\text{best},w}\}$, where w represents the total number of samples with the optimal critical aging speed. There is a strong correlation between the capacity knee points corresponding to the optimal critical speed and the cycle life.

Then, calculate the minimum and maximum values of the optimal critical aging speeds to determine the optimal critical aging speed range ($v_{\text{best,min}}, v_{\text{best,max}}$). Finally, identify the capacity knee point at which the aging speed reaches the optimal critical aging speed.

$$v_{\text{best,max}} = \max (v_{\text{best},w}) \quad (5)$$

$$v_{\text{best,min}} = \min (v_{\text{best},w}) \quad (6)$$

4. Results and Discussion

The proposed method for identifying the critical aging speed and knee points was validated on a dataset of NCM accelerated aging batteries. The optimal critical aging speed range for NCM accelerated aging batteries was found to be between $-0.032\%/cycle$ and $-0.016\%/cycle$. The correlation coefficients between the capacity knee points and cycle life extracted based on the critical aging speeds within this range were greater than 0.98. Notably, the identified optimal critical aging speed ranges were all located at the stage where the battery aging speed begins to rapidly increase, enabling the distinction between slow and rapidly increasing battery aging speed stages.

On a dataset of 123 LFP accelerated aging batteries (excluding one defective battery with a cycle life of less than 200), the proposed method for identifying the critical aging speed range and capacity knee point was verified, with a correlation coefficient threshold of 0.98. The optimal critical aging speed range for LFP accelerated aging batteries was ultimately determined to be between $-0.035\%/cycle$ and $-0.014\%/cycle$. The correlation coefficients between the capacity knee points extracted based on the critical aging speeds within this interval and the cycle life were all greater than 0.98.

As illustrated in Figure 6a, the relationship between the capacity knee point and battery cycle life of LFP batteries was identified using $-0.025\%/cycle$ as the critical aging speed. Similar to the cyclic aging characteristics of NCM lithium-ion batteries, a strong linear correlation was observed between the capacity knee point and cycle life of LFP batteries.

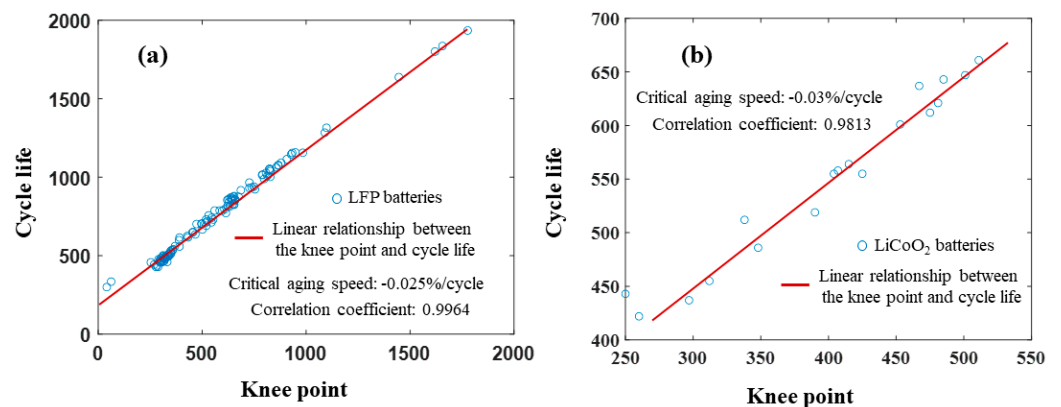


Figure 6. The linear relationship between the KP and cycle life: (a) LFP batteries; (b) LiCoO₂ batteries.

On the dataset of 18 accelerated aging LiCoO₂ batteries, the proposed method was validated, with a correlation coefficient threshold of 0.98. The optimal critical aging speed range for LiCoO₂ accelerated aging batteries was ultimately determined to be between $-0.096\%/cycle$ and $-0.03\%/cycle$. Notably, the correlation coefficients between the capacity knee points and cycle life extracted based on the critical aging speeds within this range were greater than 0.98.

As illustrated in Figure 6b, the capacity knee point corresponds to a cycle time at which the aging speed is $-0.03\%/cycle$. A strong linear correlation was observed between the capacity knee point and the cycle life of LiCoO₂ batteries, with a correlation coefficient of 0.98.

Taking into account the relationship between the capacity knee points and cycle life of NCM, LFP, and LiCoO₂ batteries, it can be observed that there is a strong linear correlation between the capacity knee point and cycle life of lithium-ion batteries across different material systems. The capacity knee point determines the cycle life and aging characteristics of accelerated aging batteries. Therefore, for the prediction of the lifespan of lithium-ion batteries, the prediction of capacity knee points and determining whether capacity knee points will occur is of great significance. Based on the critical aging speed range and capacity knee point identification method proposed in this paper, the critical aging speed ranges for NCM, LFP, and LiCoO₂ batteries with capacity knee points were determined to be $-0.032\%/cycle$ to $-0.016\%/cycle$, $-0.035\%/cycle$ to $-0.014\%/cycle$, and $-0.096\%/cycle$ to $-0.03\%/cycle$, respectively. Considering the critical aging speed ranges of the three battery material systems, the critical aging speed threshold for the capacity knee point of lithium-ion batteries is approximately $-0.03\%/cycle \pm 0.005\%/cycle$.

In ref. [1], five different capacity knee point identification methods were employed to identify the capacity knee point of accelerated aging LFP batteries, and it was found there is a linear correlation between the capacity knee point and the cycle life. The capacity knee point identification method based on the critical aging speed proposed in this paper also demonstrates a correlation coefficient close to 1 between the capacity knee point identified on the LFP battery dataset and the cycle life.

Table 3 is constructed for a better comparison between the proposed method and those reported in the ref. [1]. Compared to the identification methods of Bacon–Watts, Kneedle, bisector, quantile regression, and tangent ratio, the identification method of capacity knee point proposed in this paper fully considers the correlation between the knee point and cycle life. The proposed method is knee-point-characteristic-based, while the Bacon–Watts, Kneedle, bisector, quantile regression, and tangent ratio methods are model-based. The Bacon–Watts, Kneedle, bisector, quantile regression, and tangent ratio methods need a large amount of aging data to fit the regression model for knee point identification. After obtaining the critical aging speed threshold, the capacity diving and knee points can be determined by comparing the capacity difference between two adjacent cycles with the critical aging speed threshold. Therefore, the proposed knee point identification method can reduce the dependence on a large amount of aging data for knee point identification and capacity diving warning.

Table 3. Comparison of different knee point identification methods.

Item	Proposed Method	Bacon Watts	Kneedle	Bisector	Tangent Ratio
Method category	Knee-point-characteristic-based	Model-based	Model-based	Model-based	Model-based
Consider critical aging speed	Consider	Not	Not	Not	Not
Data requirements for real application	Few	Large	Large	Large	Large

The proposed method can be applied to different material systems including LFP, LiCoO₂, and NCM batteries, and can obtain the critical aging speed intervals of different battery material systems. By comprehensively considering the critical aging speed intervals of three material systems, the critical aging speed threshold of the lithium-ion battery knee point is about $-0.03\%/cycle \pm 0.005\%/cycle$. This empirical aging speed threshold can be used as an important reference for offline and cloud-based accelerated aging warning for lithium-ion batteries.

5. Conclusions

By analyzing the aging characteristics of accelerated aging batteries with three different material systems, it is found that there is a strong linear correlation between the capacity knee point and the cycle life of NCM batteries, LFP batteries, and LiCoO₂ batteries. This proves that the capacity knee point of lithium-ion batteries is the key factor affecting the battery cycle life. The critical aging speed interval of accelerated aging batteries and the identification method of the capacity knee point is established. By identifying the critical aging speed range and capacity knee point of accelerated aging batteries with three material systems, the critical aging speed range of accelerated aging batteries with different material systems was obtained. Considering the critical aging speed range of batteries with three material systems, the critical aging speed threshold of the capacity knee point for lithium-ion batteries is approximately $-0.03\%/cycle \pm 0.005\%/cycle$. This aging speed empirical threshold can serve as an important reference for offline and cloud-based warning systems for accelerated aging. For the diagnosis of accelerated aging in actual batteries, when the aging speed is less than $-0.03\% \pm 0.005\%/cycle$, the battery is in a relatively safe normal aging range. When the difference in the capacity retention ratio obtained from two cycle tests reaches or exceeds $-0.03\% \pm 0.005\%/cycle$, it can be considered that the battery has a high risk of accelerated aging. The research in this article reveals the important significance of the battery capacity knee point for battery life prediction and provides an important reference basis for battery accelerated aging diagnosis suitable for offline and cloud conditions.

In the future, by identifying capacity knee points, a battery's remaining life can be more accurately predicted. When a battery approaches the capacity knee point, users can be reminded to replace the battery promptly, avoiding power interruptions or performance issues at critical times. The capacity knee point identification method can help users monitor the health status of the battery in real time. When the battery capacity experiences an abnormal decline, users or systems can be alerted for repair or replacement, avoiding potential safety hazards or performance issues caused by battery malfunctions.

Author Contributions: Data curation, X.J.; formal analysis, X.J.; investigation, C.Z., L.Z. and L.Z.; methodology, X.J., C.Z., L.Z. and W.Z.; resources, W.Z. and Z.X.; software, X.J.; writing—original draft, X.J.; writing—review and editing, C.Z. and Z.X. All authors have read and agreed to the published version of the manuscript.

Funding: This research was funded by the National Key Research and Development Program of China (Grant No. 2022YFB2502304).

Institutional Review Board Statement: Not applicable.

Informed Consent Statement: Not applicable.

Data Availability Statement: The NCM experiment dataset in this paper can be found on IEEE DataPort, DOI: 10.21227/gnst-kz81. The website of the NCM battery dataset is '<https://iee-dataport.org/documents/early-diagnosis-accelerated-aging-lithium-ion-batteries-integrated-framework-ageing/>' (accessed on 27 August 2022).

Conflicts of Interest: Xinyu Jia and Zhongling Xu are employees of Sunwoda Mobility Energy Technology Co., Ltd. The paper reflects the views of the scientists, and not the company.

References

1. Attia, P.M.; Bills, A.; Brosa Planella, F.; Dechent, P.; Dos Reis, G.; Dubarry, M.; Gasper, P.; Gilchrist, R.; Greenbank, S.; Howey, D.; et al. Review—"Knees" in Lithium-Ion Battery Aging Trajectories. *J. Electrochem. Soc.* **2022**, *169*, 60517. [CrossRef]
2. Atalay, S.; Sheikh, M.; Mariani, A.; Merla, Y.; Bower, E.; Widanage, W.D. Theory of battery ageing in a lithium-ion battery: Capacity fade, nonlinear ageing and lifetime prediction. *J. Power Sources* **2020**, *478*, 229026. [CrossRef]
3. Sohn, S.; Byun, H.; Lee, J.H. CNN-based Online Diagnosis of Knee-point in Li-ion Battery Capacity Fade Curve. *IFAC-PapersOnLine* **2022**, *55*, 181–185. [CrossRef]
4. Yu, G.; Jin, Y.; Olhofer, M. A Multiobjective Evolutionary Algorithm for Finding Knee Regions Using Two Localized Dominance Relationships. *IEEE T Evol. Comput.* **2021**, *25*, 145–158. [CrossRef]

5. Liu, K.; Tang, X.; Teodorescu, R.; Gao, F.; Meng, J. Future Ageing Trajectory Prediction for Lithium-Ion Battery Considering the Knee Point Effect. *IEEE T Energy Conver* **2022**, *37*, 1282–1291. [[CrossRef](#)]
6. Han, X.; Lu, L.; Zheng, Y.; Feng, X.; Li, Z.; Li, J.; Ouyang, M. A review on the key issues of the lithium-ion battery degradation among the whole life cycle. *eTransportation* **2019**, *1*, 100005. [[CrossRef](#)]
7. Sun, S.; Guan, T.; Cheng, X.; Zuo, P.; Gao, Y.; Du, C.; Yin, G. Accelerated aging and degradation mechanism of LiFePO₄/graphite batteries cycled at high discharge rates. *RSC Adv.* **2018**, *8*, 25695–25703. [[CrossRef](#)] [[PubMed](#)]
8. Diao, W.; Kim, J.; Azarian, M.H.; Pecht, M. Degradation modes and mechanisms analysis of lithium-ion batteries with knee points. *Electrochim. Acta* **2022**, *431*, 141143. [[CrossRef](#)]
9. Yang, X.; Leng, Y.; Zhang, G.; Ge, S.; Wang, C. Modeling of lithium plating induced aging of lithium-ion batteries: Transition from linear to nonlinear aging. *J. Power Sources* **2017**, *360*, 28–40. [[CrossRef](#)]
10. Gao, Y.; Yang, S.; Jiang, J.; Zhang, C.; Zhang, W.; Zhou, X. The Mechanism and Characterization of Accelerated Capacity Deterioration for Lithium-Ion Battery with Li(NiMnCo) O₂ Cathode. *J. Electrochem. Soc.* **2019**, *166*, A1623–A1635. [[CrossRef](#)]
11. Sohn, S.; Byun, H.; Lee, J.H. Two-stage deep learning for online prediction of knee-point in Li-ion battery capacity degradation. *Appl. Energy* **2022**, *328*, 120204. [[CrossRef](#)]
12. Saxena, S.; Ward, L.; Kubal, J.; Lu, W.; Babinec, S.; Paulson, N. A convolutional neural network model for battery capacity fade curve prediction using early life data. *J. Power Sources* **2022**, *542*, 231736. [[CrossRef](#)]
13. Li, W.; Sengupta, N.; Dechent, P.; Howey, D.; Annaswamy, A.; Sauer, D.U. One-shot battery degradation trajectory prediction with deep learning. *J. Power Sources* **2021**, *506*, 230024. [[CrossRef](#)]
14. Greenbank, S.; Howey, D. Automated Feature Extraction and Selection for Data-Driven Models of Rapid Battery Capacity Fade and End of Life. *IEEE T Ind. Inf.* **2022**, *18*, 2965–2973. [[CrossRef](#)]
15. Fermín-Cueto, P.; McTurk, E.; Allerhand, M.; Medina-Lopez, E.; Anjos, M.F.; Sylvester, J.; Dos Reis, G. Identification and machine learning prediction of knee-point and knee-onset in capacity degradation curves of lithium-ion cells. *Energy AI* **2020**, *1*, 100006. [[CrossRef](#)]
16. Zhang, C.; Wang, Y.; Gao, Y.; Wang, F.; Mu, B.; Zhang, W. Accelerated fading recognition for lithium-ion batteries with Nickel-Cobalt-Manganese cathode using quantile regression method. *Appl. Energy* **2019**, *256*, 113841. [[CrossRef](#)]
17. Diao, W.; Saxena, S.; Han, B.; Pecht, M. Algorithm to Determine the Knee Point on Capacity Fade Curves of Lithium-Ion Cells. *Energies* **2019**, *12*, 2910. [[CrossRef](#)]
18. Haris, M.; Hasan, M.N.; Qin, S. Degradation Curve Prediction of Lithium-Ion Batteries Based on Knee Point Detection Algorithm and Convolutional Neural Network. *IEEE T Instrum. Meas.* **2022**, *71*, 1–10. [[CrossRef](#)]
19. Jia, X.; Zhang, C.; Wang, L.Y.; Zhang, L.; Zhou, X. Early Diagnosis of Accelerated Aging for Lithium-Ion Batteries with an Integrated Framework of Aging Mechanisms and Data-Driven Methods. *IEEE Trans. Transp. Electrif.* **2022**, *8*, 4722–4742. [[CrossRef](#)]
20. Severson, K.A.; Attia, P.M.; Jin, N.; Perkins, N.; Jiang, B.; Yang, Z.; Chen, M.H.; Aykol, M.; Herring, P.K.; Fraggedakis, D.; et al. Data-driven prediction of battery cycle life before capacity degradation. *Nat. Energy* **2019**, *4*, 383–391. [[CrossRef](#)]

Disclaimer/Publisher's Note: The statements, opinions and data contained in all publications are solely those of the individual author(s) and contributor(s) and not of MDPI and/or the editor(s). MDPI and/or the editor(s) disclaim responsibility for any injury to people or property resulting from any ideas, methods, instructions or products referred to in the content.